

# SOLUTION OF THE OECD/NEA SFR NEUTRONIC BENCHMARK USING WIMS AND MONK

**Ben Stray,\* Matthew Delaney,\* Ben Lindley, Max Shepherd,  
Simon Richards, Glynn Hosking, Peter Smith**

Amec Foster Wheeler  
Poundbury, Dorset, UK  
[ben.lindley@amecfw.com](mailto:ben.lindley@amecfw.com)

## ABSTRACT

This paper presents solutions for the Sodium Fast Reactor (SFR) benchmark defined by the OECD/NEA Working Party Scientific Issues of Reactor Systems using Amec Foster Wheeler's radiation transport codes WIMS and MONK, in order to validate these codes for SFR applications. Results for the 4 cores defined by the benchmark are presented covering medium and large concepts with metallic, oxide and carbide fuel. In particular, the innovative whole core 3D method of characteristics solver within WIMS is applied to this problem. This utilizes a once-through tracking method to ensure uniform track coverage and explicitly treat a vacuum boundary condition. In all cases, results are in good agreement with previously reported results.

*Key Words:* **Sodium-cooled fast reactor, neutronic benchmark, WIMS, MONK**

## 1. INTRODUCTION

The Generation IV International Forum defined the key research goals for advanced sodium-cooled fast reactors (SFR) as improving the safety, performance and economic competitiveness of SFR and to demonstrate a flexible management of nuclear materials, in particular, waste reduction through minor actinide burning [1]. This motivated an analysis of the transient behaviour of current SFR concepts.

This paper presents results obtained by modelling the Sodium Fast Reactor benchmark defined by the OECD/NEA Working Party Reactor and System Expert Group on Reactor Physics and Advanced Nuclear Systems, using both a Monte Carlo and deterministic approach. The codes used are MONK [2] and WIMS [3], developed by the ANSWERS team of Amec Foster Wheeler. The objectives are to validate the use of WIMS and MONK for fast reactor physics applications in view of UK and European interest in SFRs. In particular, in the final paper, the 3D method of characteristics is utilized for the deterministic transport solution. The results from both codes are compared with the values reported from the benchmark [4] [5].

As specified by the benchmark, the core multiplication factor k-effective, sodium void worth, Doppler constant, effective delayed neutron fraction, control rod worth, radial power, and the end of cycle nuclide masses are reported.

---

\* On summer placement from the University of Southampton, Southampton, UK

The benchmark specifies four different reactor designs comprising two large 3600 MWth cores, and two medium cores, generating 1000 MWth. A range of different fuels are used, namely carbide, oxide and metallic fuels. For the purpose of these models a vacuum boundary condition has been assumed, which is a good approximation. The cores consist of hexagonal subassemblies each containing either fuel, control, or shielding assemblies. The layout of each core is shown in Figure 1. The fuel zones in the medium and large cores have typical transuranic loadings of ~23% and ~14% respectively. The benchmark comprises a single cycle of 1 year, with representative equilibrium cycle compositions.

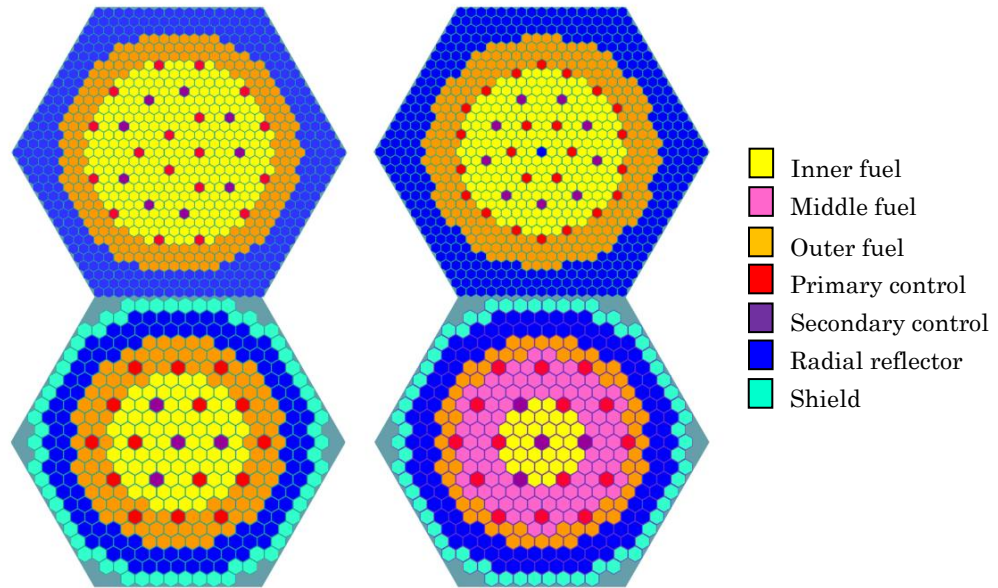


**Figure 1.** Designs for each of the cores with description of each subassembly. Clockwise from the top left: Large carbide core, large oxide core, medium oxide core, medium metallic core.

## 2. METHODS

Calculations were performed using the JEFF-3.1.2 nuclear data library.

### 2.1. WIMS

The deterministic calculations were performed using WIMS, which has a modular structure. Cell calculations were performed to generate assembly-homogenized cross sections for use in a full core calculation. The WIMS calculations were significantly faster and less computationally expensive than the MONK calculations.

The method employed to model these reactors used many of the different modules available in the WIMS code. A fine group calculation was performed using the ECCO cell code with heterogeneous cells. ECCO performs a slowing-down treatment in its fine group structure and the subgroup method. The collision probability method is used to generate flux solutions. The method of characteristics was

used to perform a 2D lattice calculation to generate assembly-homogenized cross sections (Figure 2).

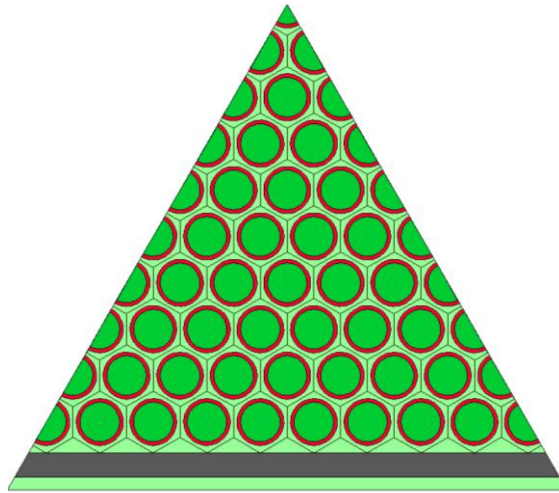


**Figure 2.** Heterogeneous representation of fuel assembly.

For the homogenisation of the control rod cells, a heterogeneous supercell model was constructed with fuel assemblies surrounding each side of the control rod (see Figure 3). The flux solution from this heterogeneous case was then used to refine the homogenized cross sections of the control rod cell such that the k-infinity and flux solution of the heterogeneous problem was reproduced (the SPH method).

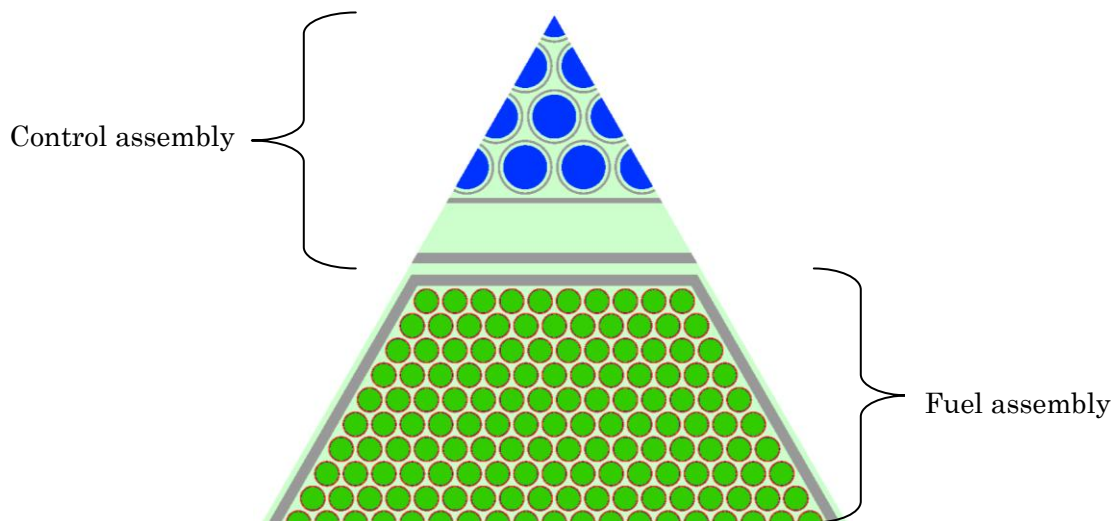


**Figure 3.** Heterogeneous geometry of control and fuel assembly prior to homogenization.

An RZ model of the core was solved using the simplified P3 (SP3) method to produce condensed 33-group cross sections. It is noted that the SP3 RZ modelling capability in WIMS allows rapid if approximate calculations to be performed for fast reactor design. Indeed it was also found that the

results of the SP3 calculation compared well with the results from the 3D transport solution and those presented in the benchmark. An additional option available within WIMS is a 3D multigroup diffusion theory solution in hexagonal-Z geometry, but this was not pursued here.

An RZ model of the core was solved using the SP3 method (Figure 4) to produce condensed 33-group cross sections. This incurred an error of 100-200 pcm, but allowed the main transport solution to be performed more rapidly. In future, it may be worthwhile to perform the SP3 calculation in a larger number of groups than 172 in order to generate more accurate 33 group cross sections for the main transport through a better representation of leakage. This would increase computational time, but the SP3 RZ calculation is nearly instantaneous, so this would be only a limited penalty.

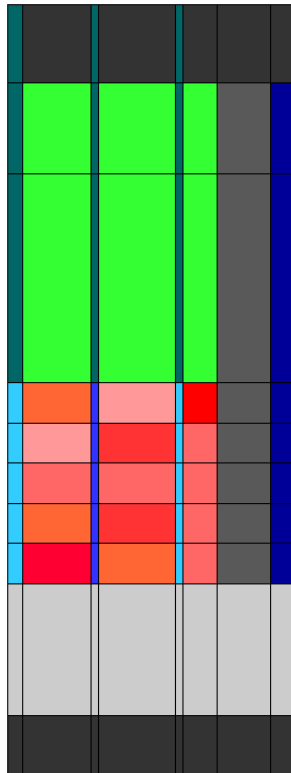


**Figure 4.** RZ model of core used in SP3 calculation

It is noted that the SP3 RZ modelling capability in WIMS allows rapid if approximate calculations to be performed for fast reactor design. Indeed it was also found that the results of the SP3 calculation compared well with the results from the 3D transport solution and those presented in the benchmark. An additional option available within WIMS is a 3D multigroup diffusion theory solution in hexagonal-Z geometry, but this was not pursued here. The capabilities of the 3D multigroup SP3 solver in WIMS are currently being extended to cover hexagonal-Z geometry.

Multigroup transport solutions are derived using the multigroup Monte Carlo method (MONK is used as a module within WIMS to provide a multigroup solution) and the 3D method of characteristics in hexagonal-Z geometry (Figure 5). A P0 transport-corrected representation of the scatter was used (i.e. adjusting total and the self scatter cross section to account for the effect of not explicitly modelling the first moment of the scatter), although at time of writing an explicit P1 representation of the scatter has

been implemented in the WIMS CACTUS method of characteristics solver, and is also available with the multigroup Monte Carlo method.

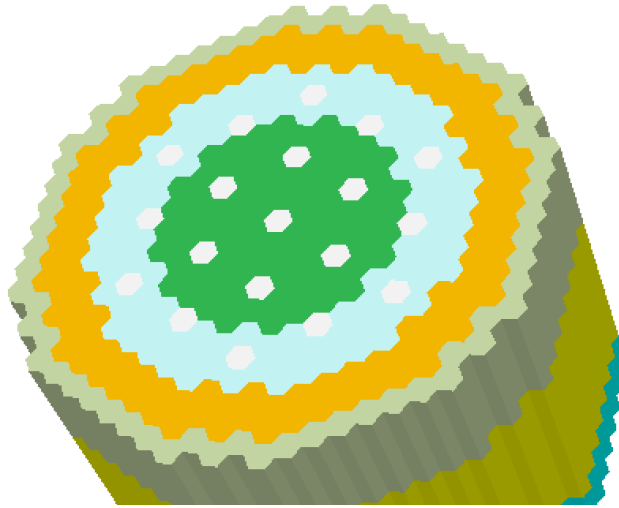


**Figure 5.** Hexagonal-Z model used for main transport solution.

The multigroup Monte Carlo calculations were performed by utilizing MONK in multigroup mode as a module within WIMS. The multigroup Monte Carlo method calculations can be run on a desktop computer, although as with continuous energy Monte Carlo, care needs to be taken to adequately converge the neutron source and a long calculation is needed to calculate distributed parameters with low statistical uncertainty.

The 3D method of characteristics solution was performed using the WIMS CACTUSOT solver. This uses a once-through tracking algorithm, where tracks are created at the core edge, pass through the core, and are terminated upon exit from the core. This method allows explicit modelling of a black boundary condition, and uniform track coverage of the model. The calculation is performed in parallel using 16 cores. Track data is prepared for each prismatic slice of the model, and the tracks are then synthesized to create tracking data for the entire 3D problem. Due to restrictions on the computational resources available, 3D method of characteristics solutions are presented for the medium-size cores only.

CACTUSOT has a great deal of geometric flexibility, so subject to computational resources (notably the memory requirements of the tracking data), a pincell homogenized or even fully explicit model of the core could be produced, to derive accurate pin-by-pin reaction rates. With an appropriate group condensation calculation, this could potentially be derived in less than 33 groups to reduce computation time.

## 2.2. MONK

MONK was used to perform Monte Carlo calculations in fully heterogeneous geometry (Figure 6). Woodcock tracking (i.e. use of pseudo-collisions rather than surface tracking) was used throughout



**Table 1.** Results for Medium Metallic Core, Beginning of Life

	<b>k-eff</b>	<b><math>\beta</math>-eff (pcm)</b>	<b><math>\Delta\rho</math> Sodium Void (pcm)</b>	<b><math>\Delta\rho</math> Doppler (pcm)</b>	<b><math>\Delta\rho</math> Control rods (pcm)</b>
<b>MONK</b>	1.0442		2282	-327	17985
<b>WIMS/CACTUSOT</b>	1.0370	345	2218	-390	19469
<b>WIMS/MONK</b>	1.0346		2070	-385	18457
<b>Benchmark (<math>\pm</math> SD)</b>	1.0354 (0.0078)	345 (10)	2024 (407)	-346 (44)	19697 (2087)

**Table 2.** Results for Medium Metallic Core, End of Life

	<b>k-eff</b>	<b><math>\beta</math>-eff (pcm)</b>	<b><math>\Delta\rho</math> Sodium Void (pcm)</b>	<b><math>\Delta\rho</math> Doppler (pcm)</b>	<b><math>\Delta\rho</math> Control rods (pcm)</b>
<b>WIMS/CACTUSOT</b>	1.0113	342	2420	-369	20524
<b>WIMS/MONK</b>	1.0092		2354	-392	19523
<b>Benchmark (<math>\pm</math> SD)</b>	1.0123 (0.0071)	344 (12)	2146 (535)	-348 (36)	20497 (2228)

**Table 3.** Results for Medium Oxide Core, Beginning of Life

	<b>k-eff</b>	<b><math>\beta</math>-eff (pcm)</b>	<b><math>\Delta\rho</math> Sodium Void (pcm)</b>	<b><math>\Delta\rho</math> Doppler (pcm)</b>	<b><math>\Delta\rho</math> Control rods (pcm)</b>
<b>MONK</b>	1.0360		1854	-733	19338
<b>WIMS/CACTUSOT</b>	1.0328	336	1972	-825	21230
<b>WIMS/MONK</b>	1.0310		1848	-766	19921
<b>Benchmark (<math>\pm</math> SD)</b>	1.0286 (0.0062)	333 (15)	1831 (228)	-730 (70)	21605 (2021)

**Table 4.** Results for Medium Oxide Core, End of Life

	<b>k-eff</b>	<b><math>\beta</math>-eff (pcm)</b>	<b><math>\Delta\rho</math> Sodium Void (pcm)</b>	<b><math>\Delta\rho</math> Doppler (pcm)</b>	<b><math>\Delta\rho</math> Control rods (pcm)</b>
<b>WIMS/CACTUSOT</b>	1.0154	332	2187	-781	21999
<b>WIMS/MONK</b>	1.0135		2079	-726	19252
<b>Benchmark (<math>\pm</math> SD)</b>	1.0136 (0.0082)	334 (13)	1922 (220)	-718 (74)	22226 (2157)

**Table 5.** Results for Large Oxide Core, Beginning of Life

	<b>k-eff</b>	<b>β-eff (pcm)</b>	<b>Δρ Sodium Void (pcm)</b>	<b>Δρ Doppler (pcm)</b>	<b>Δρ Control rods (pcm)</b>
<b>MONK</b>	1.0216		2030	-1018	5570
<b>WIMS/MONK</b>	1.0174	371	1997	-1025	6258
<b>Benchmark (± SD)</b>	1.0136 (0.0048)	369 (14)	1932 (171)	-895 (62)	6092 (995)

**Table 6.** Results for Large Oxide Core, End of Life

	<b>k-eff</b>	<b>β-eff (pcm)</b>	<b>Δρ Sodium Void (pcm)</b>	<b>Δρ Doppler (pcm)</b>	<b>Δρ Control rods (pcm)</b>
<b>WIMS/MONK</b>	1.0179	364	2188	-898	6435
<b>Benchmark (± SD)</b>	1.0183 (0.0048)	362 (14)	2021 (157)	-848 (61)	6464 (1268)

**Table 7.** Results for Large Carbide Core, Beginning of Life

	<b>k-eff</b>	<b>β-eff (pcm)</b>	<b>Δρ Sodium Void (pcm)</b>	<b>Δρ Doppler (pcm)</b>	<b>Δρ Control rods (pcm)</b>
<b>MONK</b>	1.0112		2280	-966	3980
<b>WIMS/MONK</b>	1.0054	380	2300	-1064	3811
<b>Benchmark (± SD)</b>	1.0096 (0.0090)	387 (15)	2048 (398)	-1002 (116)	4326 (1124)

**Table 8.** Results for Large Carbide Core, End of Life

	<b>k-eff</b>	<b>β-eff (pc m)</b>	<b>Δρ Sodium Void (pcm)</b>	<b>Δρ Doppler (pcm)</b>	<b>Δρ Control rods (pcm)</b>
<b>WIMS/MONK</b>	1.0200	370	2329	-950	4262
<b>Benchmark (± SD)</b>	1.0226 (0.0099)	377 (15)	2140 (238)	-930 (113)	4924 (1517)

There is in general excellent consistency between the various solutions presented here and the benchmark values. Discrepancies between solutions presented in the benchmark are due to factors such as:

- Nuclear data library. Refs [4] and [5] reported discrepancies of 600-1200 pcm for the different

cores between JEFF-3.1 and ENDF/BVII.0, with JEFF-3.1 giving a higher k-effective.

- Use of Monte Carlo or deterministic method. The deterministic method relies on multigroup cross sections, group condensation in simplified geometry and a limited angular representation of the flux and scatter.
- Representation of the fuel cells as homogeneous or heterogeneous, and with or without considering leakage through an RZ model (as in the Argonne National Laboratory code MC<sup>2</sup>-3 [6]) in the shielding calculation.
- Representation of the control cell. Ref. [4] reported that a homogeneous representation of the control cell could lead to an overestimate of the control rod worth by 10-17%.

In particular, the WIMS results can be compared to the CEA-1 results set from Refs [4] and [5]. The CEA-1 calculation scheme is very similar to that used in WIMS. The CEA-1 calculations were performed using ERANOS [7]. ECCO is used to perform a shielding calculation for heterogeneous fuel and control cells and the JEFF-3.1 data library is used (compared to the JEFF-3.1.2 data library used here). Comparison with the CEA-1 results is discussed below.

All the MONK, WIMS/CACTUSOT and WIMS/MONK calculations are within one standard deviation of the benchmark results except in the following cases:

- Some Doppler reactivities fall slightly outside of one standard deviation of the average benchmark solution, e.g. for the large oxide core beginning of life Doppler reactivity. However, in this case, the Doppler reactivity is in excellent agreement with CEA-1 (-1025 pcm for WIMS/MONK, -971 pcm for CEA-1), for which the calculation methodology is very similar. In general, both CEA-1 and WIMS predict a consistently more negative Doppler reactivity than the benchmark average, although the agreement between WIMS and CEA-1 is not in general better than the agreement between WIMS and the benchmark average for the other reactor physics parameters of interest.
- For the medium oxide core end of life control rod worth, in general the WIMS control rod worths are low compared to the benchmark. As discussed above, this is in part because many of the benchmark results use a homogeneous representation of the control cells. Even so, WIMS/MONK predicts a low worth relative to WIMS/CACTUSOT and also CEA-1. However, it is noted that the fully Monte Carlo benchmark solutions generally predict a lower rod worth than the deterministic solutions with heterogeneous control rod representation (this includes the TRIPOI-4 [8] solution provided by CEA with the JEFF-3.1 data library, which predicts a rod worth ~2000 pcm below the benchmark average in each case). Nevertheless, the WIMS/MONK calculation for end of life control rod worth for the medium oxide core is lower than all other reported solutions and warrants further analysis.
- k-effective for MONK for the medium metallic core was relatively high. To explain this, comparison is made with CEA-10 from [4]. The MONK calculations were performed with similar methodology to CEA-10 (JEFF-3.1.x nuclear data library, heterogeneous geometry representation, continuous energy Monte Carlo calculation). For the medium-sized cores (for which CEA-10 results were available) MONK and CEA-10 agreed to within 150 pcm on k-effective and 100 pcm on control rod worth, although MONK predicted a higher void reactivity.

The WIMS/CACTUSOT and WIMS/MONK k-effective calculations agree to within around 200 pcm, except for the control worth, for which WIMS/CACTUSOT predicts a value ~5% larger. In general, differences between the two cases can result from the numerical convergence and angular and mesh discretization in CACTUSOT and the source convergence and statistical convergence in MONK. Finer meshing in and around the region of the control rod may allow the flux dip in the control rod to be better resolved, and prevent potential over-prediction of the control rod worth.

The void worths predicted by WIMS and MONK are generally in good agreement with the reported values in the benchmark. This is broadly to be expected as the reported benchmark solutions report that the sensitivity of modeling assumptions to void worth is low. In particular [4] [5]:

- Shielding using a fine group scheme (as in WIMS) increases the calculated void reactivity by ~340 pcm.
- The JEFF-3.1 library (and updated versions) predicts a ~160 pcm lower void reactivity than the ENDF/BVII.0 library
- Heterogeneous cell representation lowers the calculated void worth by ~200-300 pcm.
- Many of the fully Monte Carlo solutions predict a lower void worth in some cases.

The MONK and WIMS predictions are generally in good agreement for reactivity coefficients, but there is a discrepancy of about 500 pcm in k-effective. This is thought to be due to not accounting for leakage when condensing from 1968 to 172 groups. This is consistent with similar discrepancies observed for CEA calculations in ERANOS compared to TRIPOLI [4] whereas ANL calculations which utilized a 2D RZ model in the fine group calculation had closer agreement between deterministic and Monte Carlo calculations with the fuel assembly homogenized [4]. It is anticipated that increasing the number of groups in the SP3 calculation will therefore reduce this discrepancy, and this will be performed in future work.

The agreement between reported benchmark solutions, MONK, WIMS/MONK and WIMS/CACTUSOT calculations is similar for all 4 cores, implying that the WIMS methodology can adequately be applied to cores with relatively high leakage (the medium size cores) and for different fuel forms. A full set of calculations for all 3 methodologies could ultimately be performed to help confirm this.

#### 4. CONCLUSIONS

The results reported in this paper are generally in excellent agreement with the results reported by the benchmark participants in [4] and [5]. This provides confidence in the application of WIMS and MONK to SFR reactor physics analysis. In WIMS, solutions performed using the multigroup Monte Carlo method and the CACTUSOT 3D method of characteristics solver were in good agreement with each other, continuous energy MONK and the reported results, giving confidence in the use of CACTUSOT for this application. The rod worth predicted by WIMS and MONK is generally lower than the average reported by benchmark participants, but is consistent with other solutions which use a heterogeneous representation of the control rod. Here the SPH homogenization method is used. The Doppler coefficient is generally predicted to be slightly more negative than the benchmark average, but is generally consistent with values reported using similar methodology.

## REFERENCES

- [1] D. Blanchet, L. Buiron, N. Stauff, T. K. Kim and T. Taiwo, “AEN - WPRS Sodium Fast Reactor Core Definitions (version 1.2 - September 19th),” OECD Nuclear Energy Agency, Paris, France, 2011.
- [2] S. D. Richards, C. M. J. Baker, A. J. Bird, P. Cowan, N. Davies, G. P. Dobson, T. C. Fry, A. Kyrieleis and P. N. Smith, “MONK and MCBEND: Current status and recent developments,” *Annals of Nuclear Energy*, vol. 82, pp. 68-73, 2015.
- [3] B. A. Lindley, T. D. Newton, J. G. Hosking, P. N. Smith, D. J. Powney, B. Tollit and P. J. Smith, “Release of WIMS10: A versatile reactor physics code for thermal and fast systems,” in *ICAPP2015*, Nice, France, May 3-5, 2015.
- [4] N. E. Stauff et al., “Evaluation of the Medium 1000MWth Sodium-Cooled Fast Reactor OECD Neutronic Benchmarks,” in *PHYSOR2014*, Kyoto, Japan, Sep 28 - Oct 3, 2014.
- [5] L. Burion et al., “Evaluation of the Large 3600 MWth Sodium-Cooled Fast Reactor OECD Neutronic Benchmarks,” in *PHYSOR2014*, Kyoto, Japan, Sep 28 - Oct 3, 2014.
- [6] C. H. Lee and W. S. Yang, “MC<sup>2</sup>-3: Multi-group Cross Section Generation Code for Fast Reactor Analysis,” ANL, NE-11-41, 2011.
- [7] G. Rimpault et al., “The ERANOS code and data system for fast reactor neutronic analysis,” in *PHYSOR2002*, Seoul, Korea, 2002.
- [8] TRIPOLI 4 Project Team, “TRIPOLI 4 User Guide,” CEA-R-6316 Commissariat à l’Energie Atomique et aux Energies Alternatives., 2013.